CAMBRIDGE
UNIVERSITY PRESS

Article

New arsenate minerals from the Arsenatnaya fumarole, Tolbachik volcano, Kamchatka, Russia. X. Edtollite, $K_2NaCu_5Fe^{3+}O_2(AsO_4)_4$, and alumoedtollite, $K_2NaCu_5AlO_2(AsO_4)_4$

Igor V. Pekov[1]*, Natalia V. Zubkova[1], Atali A. Agakhanov[2], Dmitry A. Ksenofontov[1], Leonid A. Pautov[2],

Evgeny G. Sidorov[3], Sergey N. Britvin[4], Marina F. Vigasina[1] and Dmitry Y. Pushcharovsky[1]

[1]Faculty of Geology, Moscow State University, Vorobievy Gory, 119991 Moscow, Russia; [2]Fersman Mineralogical Museum of the Russian Academy of Sciences, Leninsky Prospekt 18-2, 119071 Moscow, Russia; [3]Institute of Volcanology and Seismology, Far Eastern Branch of the Russian Academy of Sciences, Piip Boulevard 9, 683006 Petropavlovsk-Kamchatsky, Russia; and [4]Department of Crystallography, St Petersburg State University, University Embankment 7/9, 199034 St Petersburg, Russia

Abstract

Two new isostructural minerals edtollite $K_2NaCu_5Fe^{3+}O_2(AsO_4)_4$ and alumoedtollite $K_2NaCu_5AlO_2(AsO_4)_4$ have been found in the Arsenatnaya fumarole, Second scoria cone of the Northern Breakthrough of the Great Tolbachik Fissure Eruption, Tolbachik volcano, Kamchatka, Russia. They are associated with sylvite, tenorite, dmisokolovite, shchurovskyite, johillerite, bradaczekite, and orthoclase. Edtollite forms prismatic crystals up to 0.02 mm × 0.1 mm; alumoedtollite forms long-prismatic crystals up to 0.01 mm × 0.1 mm. Both minerals have a semi-metallic lustre. Edtollite is brown–black to black and alumoedtollite is bronze coloured. $D_{calc.}$ = 4.26 (edtollite) and 4.28 (alumoedtollite) g cm^{-3}. In reflected light, both minerals are grey, with distinct anisotropy. Reflectance values [edtollite/alumoedtollite: R_1–R_2, % (λ, nm)] are: 8.3–8.2/8.7–7.7 (470); 7.7–7.4/8.3–7.4 (546); 7.1–6.9/8.3–7.4 (589); and 6.3–6.3/7.6–7.2 (650). Chemical data are: (edtollite/alumoedtollite, wt.%, electron-microprobe): Na$_2$O 3.13/2.58, K$_2$O 8.12/9.09, Rb$_2$O 0.00/0.11, CaO 0.00/0.52, CuO 36.55/38.35, ZnO 0.46/0.00, Al$_2$O$_3$ 0.00/3.48, Fe$_2$O$_3$ 7.34/1.79, TiO$_2$ 0.27/0.00, As$_2$O$_5$ 43.57/43.66, total 99.44/99.58. The empirical formulae, based on 18 O apfu, for edtollite is: $K_{1.83}Na_{1.07}Cu_{4.88}Zn_{0.06}Fe^{3+}_{0.98}Ti_{0.04}As_{4.03}O_{18}$; and for alumoedtollite is: $K_{2.02}Rb_{0.01}Na_{0.87}Ca_{0.10}Cu_{5.06}Al_{0.72}Fe^{3+}_{0.24}As_{3.99}O_{18}$. Both minerals are triclinic, $P\bar{1}$; unit-cell parameters (edtollite/alumoedtollite) are: a = 5.1168(6)/5.0904(11), b = 9.1241(12)/9.0778(14), c = 9.6979(14)/9.6658(2) Å, α = 110.117(13)/110.334(17), β = 102.454(12)/102.461(19), γ = 92.852(11)/92.788(15)°, V = 411.32(9)/404.88(14) Å^3 and Z = 1/1. The strongest reflections in the powder X-ray diffraction pattern [d, Å(I)(hkl)] are for edtollite: 8.79(92)(001), 7.63(41)(0$\bar{1}$1), 5.22(44)(011), 3.427(100)(012), 3.148(64)(0$\bar{1}$3), 2.851(65)($\bar{1}$03) and 2.551(40)($\bar{2}$01); and for alumoedtollite: 8.78(81)(001), 7.62(67)(0$\bar{1}$1), 3.418(100)(012), 3.147(52)(0$\bar{1}$3), 2.558(58)($\bar{1}$22), 2.544(65)($\bar{2}$01) and 2.528(52)($\bar{1}\bar{3}$2). The crystal structures [single-crystal X-ray diffraction, R = 0.0773 (edtollite) and 0.0826 (alumoedtollite); 1504 and 1046 unique reflections, respectively] represent a novel structure type. It is based upon a heteropolyhedral pseudo-framework with the column formed by Cu^{2+}-centred octahedra and square pyramids, octahedra MO_6 (M = Fe^{3+}, Al^{3+} or Cu^{2+}) and AsO$_4$ tetrahedra as the main building unit. K$^+$ and Na$^+$ are located in wide and narrow channels, respectively. Edtollite is named after the Russian geologist and Arctic explorer Eduard Vasilievich Toll (1858–1902), alumoedtollite is its analogue with Al prevailing among trivalent cations.

Introduction

This is the tenth contribution to our series of papers on new arsenate minerals from the Arsenatnaya fumarole located at the apical part of the Second scoria cone of the Northern Breakthrough of the Great Tolbachik Fissure Eruption, Tolbachik volcano, Kamchatka Peninsula, Far-Eastern Region, Russia (55°41'N, 160° 14'E, 1200 m asl). This active fumarole, discovered by us in July 2012, was characterised by Pekov *et al.* (2014*a*, 2018*b*). Previous papers described yurmarinite Na$_7$(Fe^{3+},Mg,Cu)$_4$(AsO$_4$)$_6$ (Pekov *et al.*, 2014*a*), two polymorphs of Cu$_4$O(AsO$_4$)$_2$, ericlaxmanite and kozyrevskite (Pekov *et al.*, 2014*b*), popovite Cu$_5$O$_2$(AsO$_4$)$_2$ (Pekov *et al.*, 2015*b*), structurally related shchurovskyite K$_2$CaCu$_6$O$_2$(AsO$_4$)$_4$ and dmisokolovite K$_3$Cu$_5$AlO$_2$(AsO$_4$)$_4$ (Pekov *et al.*, 2015*c*), katiarsite KTiO(AsO$_4$) (Pekov *et al.*, 2016*a*), melanarsite K$_3$Cu$_7$Fe^{3+}O$_4$(AsO$_4$)$_4$ (Pekov *et al.*, 2016*d*), pharmazincite KZnAsO$_4$ (Pekov *et al.*, 2017*a*), arsenowagnerite Mg$_2$(AsO$_4$)F (Pekov *et al.*, 2018*a*) and arsenatrotitanite NaTiO(AsO$_4$) (Pekov *et al.*, 2018*c*).

In this paper we describe two isostructural new minerals: edtollite (Cyrillic: эдтоллит), ideally K$_2$NaCu$_5$Fe^{3+}O$_2$(AsO$_4$)$_4$ and alumoedtollite (алюмоэдтоллит), ideally K$_2$NaCu$_5$AlO$_2$(AsO$_4$)$_4$. Edtollite is named in honour of the Russian geologist and Arctic

*Author for correspondence: Igor V. Pekov, Email: igorpekov@mail.ru
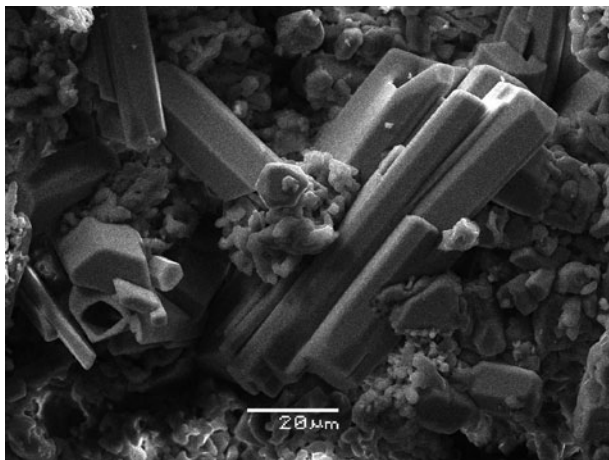
Fig. 1. Near-parallel intergrowths of edtollite crystals on a crystal crust mainly consisting of As-bearing orthoclase and sylvite. Scanning electron microscopy (secondary electron) image.
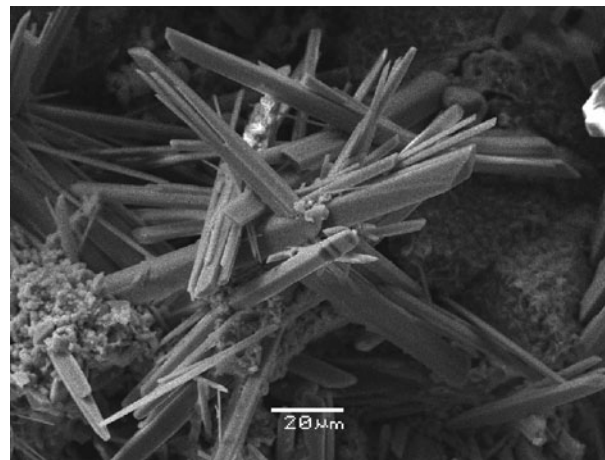
Fig. 3. Clusters of long-prismatic crystals of alumoedtollite on sylvite crust. Scanning electron microscopy (secondary electron) image.
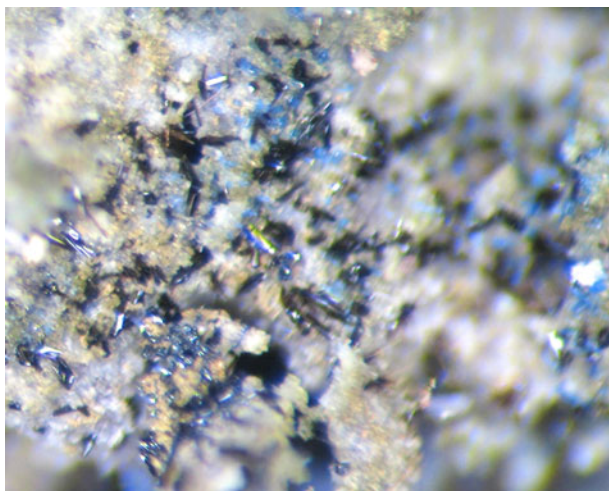
Fig. 2. Black prismatic crystals of edtollite on a crust mainly consisting of colourless As-bearing orthoclase and sylvite, with blue bradaczekite. Field of view: 1.2 mm wide. Photo: I.V. Pekov and A.V. Kasatkin.
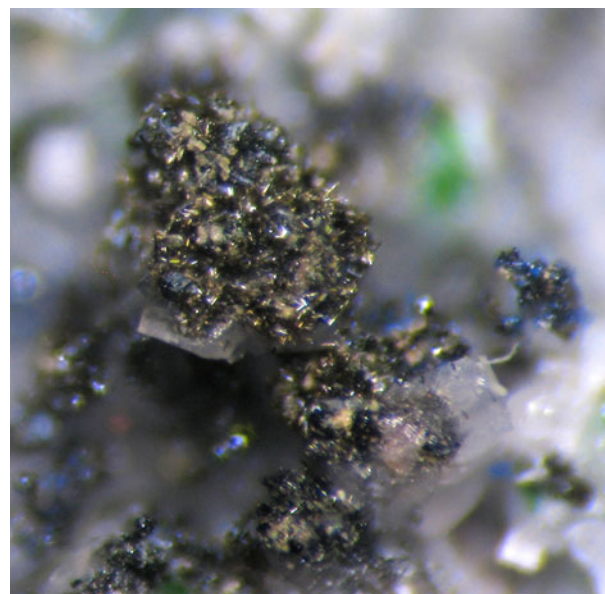
Fig. 4. Aggregates of small bronze-coloured prismatic crystals of alumoedtollite close associated with green dmisokolovite, blue bradaczekite, black tenorite and colourless sylvite. Field of view 1.8 mm wide. Photo: I.V. Pekov and A.V. Kasatkin.

explorer Eduard Vasilievich Toll (1858–1902) who made significant contributions to the geology and geography of Polar Siberia and islands in the Arctic Ocean. He had German roots and is also known as Eduard Gustav von Toll. Alumoedtollite is named as an analogue of edtollite with aluminium prevailing among trivalent cations (Al > Fe^{3+}). Both new minerals and their names have been approved by the IMA Commission on New Minerals, Nomenclature and Classification (CNMNC); IMA2016–010 (edtollite, Pekov *et al.*, 2016*c*) and IMA2017–020 (alumoedtollite, Pekov *et al.*, 2017*b*). The type specimens are deposited in the systematic collection of the Fersman Mineralogical Museum of the Russian Academy of Sciences, Moscow, with the catalogue numbers 95350 (edtollite) and 95906 (alumoedtollite).

Occurrence and general appearance

Specimens with both new minerals were collected by us in July 2015 at the northern area of the Arsenatnaya fumarole, from

the depth of 1 m under the day surface. The temperature measured using a chromel–alumel thermocouple during collecting was 420°C in this pocket. We believe that edtollite and alumoedtollite were deposited directly from the gas phase as volcanic sublimates at temperatures not lower than 420–450°C.

Edtollite and alumoedtollite belong to the rarest Tolbachik minerals, found in negligible amounts: the former was identified in two small specimens and the latter in only one specimen. They occur in polymineralic assemblages. Edtollite is associated with orthoclase (As-bearing), sylvite, halite, hematite, tenorite, bradaczekite, johillerite, dmisokolovite, shchurovskyite, lammerite, ericlaxmanite, yurmarinite, popovite, arsmirandite (IMA2014–081, Pekov *et al.*, 2015*a*), pharmazincite, tilasite, svabite, hatertite, nickenichite, durangite, aphthitalite, langbeinite, calciolangbeinite, anhydrite, wulffite, euchlorine, alumoklyuchevskite, krasheninnikovite, wulfenite, fluoborite, cassiterite,

Table 1. Reflectance data (R, %) for edtollite and alumoedtollite.

λ (nm)	Edtollite		Alumoedtollite		λ (nm)	Edtollite		Alumoedtollite	
	R_1	R_2	R_1	R_2		R_1	R_2	R_1	R_2
400	7.0	6.8	9.1	8.0	560	7.6	7.3	8.3	7.4
420	7.1	7.2	9.0	7.9	580	7.2	7.0	8.3	7.4
440	7.8	7.8	8.8	7.8	**589**	**7.1**	**6.9**	**8.3**	**7.4**
460	8.1	8.2	8.7	7.7	600	6.9	6.8	8.3	7.4
470	**8.3**	**8.2**	**8.7**	**7.7**	620	6.6	6.5	8.2	7.3
480	8.4	8.2	8.6	7.7	640	6.4	6.3	7.6	7.3
500	8.2	7.9	8.3	7.6	**650**	**6.3**	**6.3**	**7.6**	**7.2**
520	8.0	7.7	8.3	7.5	660	6.3	6.2	7.6	7.1
540	7.8	7.5	8.3	7.5	680	6.2	6.2	7.6	7.0
546	**7.7**	**7.4**	**8.3**	**7.4**	700	6.3	6.4	7.6	7.0

Data for wavelengths recommended by the IMA Commission on ore microscopy (COM) are marked in boldtype.
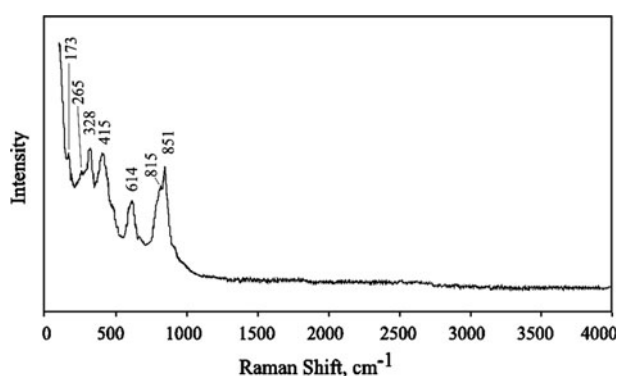
Fig. 5. The Raman spectrum of edtollite.

Table 2. Average chemical composition (wt.%, ranges are in parentheses) of edtollite and alumoedtollite.

Constituent	Edtollite	Alumoedtollite	Probe standard
Na_2O	3.13 (2.54–3.64)	2.58 (2.32–2.91)	Albite
K_2O	8.12 (8.03–8.29)	9.09 (8.96–9.22)	Microcline
Rb_2O	–	0.11 (0.00–0.47)	$RbNb_4O_{11}$
CaO	–	0.52 (0.32–0.76)	Wollastonite
CuO	36.55 (35.35–38.40)	38.35 (37.75–38.88)	Cu
ZnO	0.46 (0.00–1.13)	–	ZnS
Al_2O_3	–	3.48 (3.22–3.81)	Al_2O_3
Fe_2O_3	7.34 (6.56–8.59)	1.79 (1.34–2.30)	Magnetite
TiO_2	0.27 (0.00–0.62)	–	Ilmenite
As_2O_5	43.57 (42.34–44.43)	43.66 (42.94–44.60)	InAs
Total	99.44	99.58	

'–' = below detection limit.

rutile, pseudobrookite and fluorophlogopite. In close association with alumoedtollite is sylvite, halite, tenorite, dmisokolovite, shchurovskyite, arsmirandite, johillerite, bradaczekite, tilasite, orthoclase (As-bearing), hematite and anhydrite.

Edtollite occurs as prismatic crystals up to 0.02 mm × 0.02 mm × 0.1 mm, their near-parallel (Fig. 1) or chaotic intergrowths up to 0.3 mm across. Rarely its crystals form, together with prismatic crystals of As-bearing orthoclase, open-work aggregates up to 1 mm across. In close association with bradaczekite, johillerite, dmisokolovite and hematite, the new mineral overgrows incrustations mainly consisting of As-bearing orthoclase and sylvite (Figs 1 and 2) that covers basalt scoria altered by fumarolic gas.

Late-generation sylvite overgrows all the minerals listed. Alumoedtollite occurs as long-prismatic to acicular crystals up to 0.01 mm × 0.01 mm × 0.1 mm, forming bush-like clusters and open-work aggregates (up to 1 mm across) together with other arsenates, tenorite and sylvite (Figs 3 and 4).

Physical properties and optical data

Both new minerals are translucent to almost opaque, with a semi-metallic lustre. Edtollite is brown–black to black, some crystals have an olive-green hue, and the streak is light brown. Alumoedtollite is bronze coloured with a light yellow streak. Both minerals are brittle, cleavage or parting was not observed, and the fracture is uneven (observed under the scanning electron microscope). The Mohs' hardness and density could not be measured because of the small size of crystals and the open-work character of aggregates. Density values calculated using the empirical formulae and the unit-cell parameters from single-crystal X-ray diffraction data are 4.264 g cm^{-3} for edtollite and 4.280 g cm^{-3} for alumoedtollite.

Optical properties of the new minerals were examined in reflected light. Both are grey, and pleochroism was not observed. Anisotropism is distinct. Bireflectance is very weak for edtollite ($\Delta R = 0.2\%$) and weak for alumoedtollite ($\Delta R = 0.9\%$) (589 nm). Internal reflections are weak, brown for edtollite and yellowish for alumoedtollite. The reflectance values for both minerals measured by means of the UMSP-50 Opton microspectrophotometer using the SiC standard are given in Table 1.

Raman spectroscopy

The Raman spectrum of edtollite (Fig. 5) was obtained on a crystal cluster using an EnSpectr R532 instrument (Dept. of Mineralogy, Moscow State University) with a green laser (532 nm) at room temperature. The output power of the laser beam was ~15 mW. The spectrum was processed using the *EnSpectr* expert mode program in the range from 100 to 4000 cm^{-1} with the use of a holographic diffraction grating with 1800 lines cm^{-1} and a resolution of 6 cm^{-1}. The diameter of the focal spot on the sample was ~10 μm. The back-scattered Raman signal was collected with 40× objective; signal acquisition time for a single scan of the spectral range was 1000 ms and the signal was averaged over 50 scans.

The strong band with maximum at 851 cm^{-1} (with a shoulder at 815 cm^{-1}) corresponds to As^{5+}–O stretching vibrations of

Table 3. Powder X-ray diffraction data (*d* in Å) for edtollite.

*I*_obs	*I*_calc*	*d*_obs	*d*_calc**	*h k l*
92	**100**	**8.79**	**8.821**	**0 0 1**
3	2	8.50	8.489	0 1 0
41	**97**	**7.63**	**7.667**	**0 $\bar{1}$ 1**
44	**27**	**5.22**	**5.238**	**0 1 1**
2	13	4.93	4.951	1 0 0
16	20	4.84	4.863	$\bar{1}$ 0 1
21	22	4.65	4.670	0 $\bar{1}$ 2
7	6, 2	4.55	4.553, 4.521	$\bar{1}$ 1 0, 0 $\bar{2}$ 1
11	6	4.39	4.411	0 0 2
36	44	4.34	4.348	$\bar{1}$ $\bar{1}$ 1
17	10	4.23	4.244	0 2 0
9	7	3.784	3.794	$\bar{1}$ 0 2
100	**59**	**3.427**	**3.436**	**0 1 2**
26	11, 23	3.362	3.375, 3.366	0 2 1, 1 $\bar{2}$ 1
5	10	3.298	3.311	$\bar{1}$ $\bar{2}$ 1
64	**44**	**3.148**	**3.156**	**0 $\bar{1}$ 3**
19	15	3.090	3.096	$\bar{1}$ 2 1
25	34	3.016	3.026	1 2 0
36	31	2.942	2.950	1 0 2
30	20, 27	2.897	2.911, 2.902	0 $\bar{3}$ 2, 1 $\bar{2}$ 2
65	**45**	**2.851**	**2.859**	**$\bar{1}$ 0 3**
9	8	2.738	2.748	$\bar{1}$ $\bar{2}$ 3
34	38	2.651	2.659	1 $\bar{3}$ 1
33	15, 8	2.612	2.619, 2.614	0 2 2, $\bar{1}$ 3 0
77	**54, 24**	**2.569**	**2.574, 2.558**	**$\bar{1}$ 2 2, 1 2 1**
40	**70**	**2.551**	**2.554**	**$\bar{2}$ 0 1**
38	**51, 2**	**2.528**	**2.536, 2.521**	**1 $\bar{3}$ 2, $\bar{1}$ $\bar{3}$ 1**
11	3	2.475	2.482	1 $\bar{3}$ 2
9	11, 2	2.457	2.468, 2.448	$\bar{2}$ 1 0, 0 3 1
13	7	2.430	2.433	1 $\bar{1}$ 3
9	11	2.385	2.391	1 $\bar{2}$ 3
30	37	2.355	2.363	$\bar{1}$ $\bar{3}$ 3
6	7, 4	2.331	2.335, 2.325	0 $\bar{2}$ 4, 1 3 0
5	5, 2	2.290	2.297, 2.294	$\bar{2}$ 1 2, 2 $\bar{1}$ 1
6	10	2.279	2.284	$\bar{1}$ $\bar{2}$ 4
4	6	2.254	2.260	0 $\bar{4}$ 2
6	3	2.221	2.222	$\bar{2}$ 2 1
23	13	2.202	2.205	0 0 4
7	2	2.170	2.174	$\bar{2}$ $\bar{2}$ 2
8	13	2.158	2.162	0 3 4
16	3, 5, 10	2.116	2.122, 2.120, 2.116	0 4 0, 1 $\bar{4}$ 1, $\bar{1}$ 2 3
6	2, 2	2.084	2.092, 2.088	$\bar{1}$ $\bar{3}$ 4, 0 2 3
6	4	2.065	2.070	$\bar{1}$ 3 2
12	8, 33	2.034	2.038, 2.034	$\bar{2}$ 1 3, 2 $\bar{1}$ 2
6	4	1.964	1.967	0 1 4
4	2	1.955	1.959	1 $\bar{1}$ 4
4	2	1.935	1.940	$\bar{2}$ $\bar{1}$ 4
6	5	1.895	1.898	$\bar{1}$ 4 1
2	2	1.882	1.885	$\bar{2}$ $\bar{2}$ 4
7	6	1.858	1.862	1 4 0
5	5, 6	1.827	1.830, 1.827	$\bar{2}$ 2 3, 2 2 1
6	7, 2	1.784	1.785, 1.781	$\bar{2}$ 3 2, $\bar{1}$ 3 3
9	1, 7	1.772	1.775, 1.771	1 3 2, 2 $\bar{1}$ 3
15	16	1.716	1.718	0 2 4
17	17, 7, 4, 3	1.694	1.698, 1.697, 1.693, 1.693	0 5 0, 2 0 3, $\bar{2}$ $\bar{1}$ 5, 0 $\bar{4}$ 5
5	3, 2, 3	1.683	1.688, 1.686, 1.683	0 4 2, 1 4 1, 2 $\bar{4}$ 2
4	7	1.658	1.657	$\bar{3}$ $\bar{1}$ 2
7	8	1.640	1.642	$\bar{2}$ 0 5
18	9, 6, 1, 1	1.623	1.627, 1.625, 1.622, 1.621	1 $\bar{1}$ 5, 1 $\bar{3}$ 5, 2 2 2, $\bar{3}$ 0 3
7	7	1.601	1.604	$\bar{2}$ $\bar{3}$ 5
2	2, 2, 1	1.566	1.570, 1.570, 1.569	$\bar{1}$ 5 1, $\bar{3}$ $\bar{2}$ 2, $\bar{3}$ 2 2
2	5, 1	1.556	1.559, 1.557	3 $\bar{2}$ 1, 0 $\bar{3}$ 6
5	5, 1	1.544	1.546, 1.545	0 $\bar{1}$ 6, 1 0 5
11	2, 11, 12, 2, 3	1.539	1.542, 1.542, 1.541, 1.539, 1.537	$\bar{2}$ 1 5, $\bar{3}$ $\bar{2}$ 1, 1 $\bar{4}$ 5, 1 3 3, $\bar{1}$ 3 4
6	9, 5	1.512	1.514, 1.511	3 0 4, 1 2 4
5	4	1.505	1.507	0 $\bar{6}$ 3
7	8, 3, 6	1.493	1.499, 1.498, 1.491	$\bar{1}$ 2 5, 2 $\bar{5}$ 2, $\bar{1}$ $\bar{4}$ 6
5	10, 4, 7	1.481	1.484, 1.481, 1.478	0 $\bar{6}$ 1, $\bar{3}$ 2 3, $\bar{2}$ $\bar{1}$ 6
3	2	1.459	1.462	1 $\bar{6}$ 1
7	4, 3	1.453	1.455, 1.451	0 $\bar{6}$ 4, 2 $\bar{4}$ 4

(Continued)

Table 3. (*Continued.*)

I_obs	I_calc*	d_obs	d_calc**	h k l
6	2, 6, 4	1.434	1.437, 1.437, 1.434	2 5̄ 3, 2̄ 5 1, 2 2 3
6	3	1.432	1.432	1 1 5
3	8, 1, 2	1.416	1.417, 1.417, 1.415	2̄ 2 5, 2̄ 4 3, 3̄ 3̄ 1
3	4	1.403	1.406	1̄ 6̄ 4
2	4, 5, 7	1.392	1.397, 1.394, 1.392	3̄ 4 0, 3̄ 2̄ 5, 2̄ 5̄ 1
2	1	1.388	1.389	0 5̄ 6
2	4, 2	1.380	1.383, 1.380	1̄ 5̄ 6, 2 1 4
3	2	1.372	1.374	0 6̄ 5
3	2, 1, 3	1.366	1.367, 1.367, 1.367	0 1 6, 1 4̄ 6, 3̄ 3 3
3	3, 2	1.347	1.348, 1.348	2 1̄ 5, 0 3̄ 7
1	2	1.329	1.329	2 6̄ 2
1	4, 1	1.320	1.321, 1.318	3̄ 4 2, 0 1̄ 7
6	2, 8, 1	1.305	1.308, 1.307, 1.304	1 2 5, 2̄ 6 0, 1 6̄ 5
3	1, 3, 3, 1, 2	1.295	1.297, 1.297, 1.296, 1.293, 1.293	1̄ 2 6, 2 6̄ 3, 1 5̄ 6, 2 3 3, 2 0 5

*For the calculated pattern, only reflections with intensities ≥1 are given; **for the unit-cell parameters calculated from single-crystal data.
The strongest lines are given in bold.

Table 4. Powder X-ray diffraction data (d in Å) for alumoedtollite.

I_obs	I_calc*	d_obs	d_calc**	h k l
81	**100**	**8.78**	**8.772**	**0 0 1**
67	**94**	**7.62**	**7.640**	**0 1̄ 1**
48	**31**	**5.20**	**5.200**	**0 1 1**
10	18	4.835	4.838	1̄ 0 1
23	23	4.653	4.653	0 1̄ 2
22	50	4.326	4.329	1̄ 1̄ 1
26	14	4.214	4.217	0 2 0
7	1	4.030	4.023	1 1 0
13	4	3.903	3.901	1 0 1
19	9	3.768	3.774	1̄ 0 2
100	**4, 67**	**3.418**	**3.441, 3.412**	**1̄ 2 0, 0 1 2**
42	14, 29	3.352	3.351, 3.350	0 2 1, 1 2̄ 1
15	11	3.294	3.295	1̄ 2̄ 1
52	**17, 50**	**3.147**	**3.166, 3.143**	**1̄ 2 2, 0 1̄ 3**
15	17	3.072	3.074	1̄ 2 1
30	39	3.008	3.009	1 2 0
19	7	2.956	2.956	1̄ 1̄ 3
24	34	2.941	2.933	1 0 2
37	21, 28	2.895	2.899, 2.890	0 3̄ 2, 1 2̄ 2
51	**49**	**2.843**	**2.843**	**1̄ 0 3**
16	9	2.738	2.738	1̄ 2̄ 3
32	42	2.645	2.645	1 3̄ 1
35	14, 9	2.605	2.600, 2.597	0 2 2, 1̄ 3 0
58	**58**	**2.558**	**2.556**	**1̄ 2 2**
65	**2, 26, 76**	**2.544**	**2.547, 2.542, 2.541**	**0 3̄ 3, 1 2 1, 2̄ 0 1**
52	**55**	**2.528**	**2.526**	**1 3̄ 2**
18	2, 7	2.428	2.430, 2.422	0 3 1, 1 1̄ 3
30	3, 40	2.355	2.360, 2.354	1̄ 3 1, 1̄ 3̄ 3
13	4, 7	2.333	2.331, 2.326	1̄ 1̄ 4, 0 2̄ 4
11	2, 11	2.278	2.282, 2.276	2 1̄ 1, 1̄ 2̄ 4
11	8	2.251	2.250	0 4̄ 2
16	4, 12	2.196	2.209, 2.193	2̄ 2 1, 0 0 4
14	15	2.155	2.155	0 3̄ 4
23	6, 5, 6	2.110	2.118, 2.109, 2.108	0 4̄ 3, 0 4 0, 1 4̄ 1
10	2, 2	2.077	2.085, 2.073	1̄ 3 4, 0 2 3
22	4, 3	2.055	2.055, 2.050	1̄ 3 2, 2 1 1
18	4, 1, 9, 35	2.028	2.034, 2.029, 2.026, 2.024	1̄ 4̄ 2, 1 1 3, 2̄ 1 3, 2 1̄ 2
10	4, 2	1.953	1.955, 1.950	0 1 4, 1 1̄ 4
14	7	1.884	1.885	1̄ 4 1
8	8	1.849	1.850	1 4 0
8	5, 6	1.820	1.818, 1.817	2̄ 2 3, 2 2 1
8	5	1.780	1.782	0 5̄ 1
11	7, 6, 2	1.771	1.773, 1.769, 1.768	2̄ 3 2, 0 5̄ 3, 1̄ 3 3
12	16	1.709	1.706	0 2 4
22	6, 7, 4, 18, 3	1.689	1.693, 1.688, 1.687, 1.687, 1.685	2 3̄ 3, 2 0 3, 0 4̄ 5, 0 5 0, 2̄ 1̄ 5

(*Continued*)

Table 4. (*Continued.*)

I_{obs}	I_{calc}*	d_{obs}	d_{calc}**	$h \, k \, l$
11	3	1.662	1.665	$0 \, \bar{5} \, 4$
9	9, 5	1.620	1.619, 1.618	$1 \, \bar{1} \, 5, \, 1 \, \bar{3} \, 5$
6	3	1.605	1.605	$\bar{3} \, 2 \, 0$
6	1, 7	1.600	1.602, 1.598	$\bar{2} \, 3 \, 3, \, \bar{2} \, \bar{3} \, 5$
9	7	1.582	1.579	$\bar{1} \, \bar{1} \, 6$
7	4, 2	1.566	1.567, 1.563	$\bar{1} \, \bar{3} \, 6, \, \bar{3} \, \bar{2} \, 2$
12	4, 1, 12, 11	1.537	1.539, 1.536, 1.536, 1.534	$0 \, \bar{1} \, 6, \, 1 \, 0 \, 5, \, 1 \, \bar{4} \, 5, \, \bar{3} \, \bar{2} \, 1$
7	1, 17, 2	1.509	1.509, 1.509, 1.507	$0 \, \bar{6} \, 2, \, \bar{3} \, 3 \, 0, \, \bar{1} \, 0 \, 6$
6	4, 7, 6	1.489	1.491, 1.489, 1.486	$2 \, \bar{5} \, 2, \, \bar{1} \, 2 \, 5, \, \bar{1} \, \bar{4} \, 6$
10	2, 1, 11, 4	1.476	1.480, 1.478, 1.475, 1.472	$\bar{3} \, \bar{2} \, 4, \, \bar{2} \, \bar{2} \, 6, \, 0 \, \bar{6} \, 1, \, \bar{3} \, 2 \, 3$
6	4, 9, 3, 5	1.444	1.445, 1.443, 1.442, 1.441	$2 \, \bar{4} \, 4, \, \bar{3} \, \bar{3} \, 3, \, 1 \, \bar{6} \, 3, \, \bar{3} \, 3 \, 2$
6	7, 5, 4	1.426	1.427, 1.425, 1.423	$\bar{2} \, 5 \, 1, \, 2 \, 2 \, 3, \, 1 \, 1 \, 5$
6	1, 5	1.402	1.404, 1.400	$\bar{3} \, \bar{1} \, 5, \, \bar{1} \, \bar{6} \, 4$
4	8, 4	1.381	1.384, 1.378	$\bar{2} \, \bar{5} \, 1, \, \bar{1} \, \bar{5} \, 6$
5	2, 2, 2	1.343	1.345, 1.343, 1.342	$2 \, \bar{5} \, 4, \, 0 \, \bar{2} \, 7, \, 0 \, \bar{3} \, 7$
12	10, 1, 2, 3, 4	1.294	1.299, 1.299, 1.293, 1.292, 1.292	$\bar{2} \, 6 \, 0, \, 1 \, \bar{6} \, 5, \, \bar{2} \, \bar{1} \, 7, \, 1 \, \bar{5} \, 6, \, 1 \, 5 \, 2$
9	1, 4, 3, 2	1.225	1.228, 1.226, 1.225, 1.224	$\bar{4} \, 2 \, 2, \, \bar{1} \, \bar{7} \, 2, \, 3 \, \bar{3} \, 4, \, 2 \, 5 \, 1$

*For the calculated pattern, only reflections with intensities ≥1 are given; **for the unit-cell parameters calculated from single-crystal data.
The strongest lines are given in bold.

Table 5. Crystal data, data collection information and structure refinement details for edtollite and alumoedtollite.

Mineral	Edtollite	Alumoedtollite
Crystal data		
Formula	$K_{1.8}NaCu_4(Fe^{3+}_{1.2}Cu_{0.8})O_2(AsO_4)_4$	$K_2(Na_{0.9}Ca_{0.1})Cu_4(Cu_{1.1}Al_{0.7}Fe^{3+}_{0.2})O_2(AsO_4)_4$
Crystal size (mm)	0.01 × 0.02 × 0.04	0.01 × 0.01 × 0.02
Crystal system, space group, Z	Triclinic, $P\bar{1}$, 1	
Temperature (K)	293(2)	
a, b, c (Å)	5.1168(6), 9.1241(12), 9.6979(14)	5.0904(11), 9.0778(14), 9.6658(2)
α, β, γ (°)	110.117(13), 102.454(12), 92.852(11)	110.334(17), 102.461(19), 92.788(15)
V (Å³)	411.32(9)	404.88(14)
Calculated density (g cm⁻³)	4.264	4.280
Formula weight	1053.06	1044.69
μ (mm⁻¹)	15.687	15.579
Data collection		
Diffractometer	Xcalibur S CCD	
Radiation, wavelength (Å)	Mo$K\alpha$; 0.71073	
F_{000}	492	488
θ range for data collection (°)	2.66–28.28	3.92–28.28
Absorption correction	Multi-scan; Empirical absorption correction using spherical harmonics, implemented in *SCALE3 ABSPACK* scaling algorithm.	
Reflections collected	6423	6270
Independent reflections	2036 (R_{int} = 0.1118)	2014 (R_{int} = 0.1654)
Independent reflections with $I > 2\sigma(I)$	1504	1046
Index ranges	$-6 \leq h \leq 6, \, -12 \leq k \leq 12, \, -12 \leq l \leq 12$	
Refinement		
Data reduction	*CrysAlisPro*, Agilent Technologies, Version 1.171.37.35 (Agilent Technologies, 2014)	
Structure solution/refinement method	Direct methods/ full-matrix least-squares on F^2	
Number of refined parameters	134	137
Final R indices [$I > 2\sigma(I)$]	R_1 = 0.0773, wR_2 = 0.1395	R_1 = 0.0826, wR_2 = 0.1707
R indices (all data)	R_1 = 0.1112, w$R2$ = 0.1533	R_1 = 0.1708, wR_2 = 0.2187
GoF	1.084	0.946
$\Delta\rho_{max}, \Delta\rho_{min}$ (e– Å–3)	2.27 and –1.47	2.48 and –1.97

AsO_4^{3-} anionic groups. Bands with frequencies <700 cm⁻¹ correspond to bending vibrations of AsO_4 tetrahedra, Cu^{2+}–O and Fe^{3+}–O stretching vibrations and lattice modes. The absence of bands with frequencies >900 cm⁻¹ indicates the absence of groups with O–H, C–H, C–O, N–H, N–O and B–O bonds in the mineral.

Chemical composition

Chemical data for both new minerals were obtained using a Jeol 733 electron microprobe instrument (wavelength-dispersive mode, acceleration voltage of 20 kV, beam current of 20 nA and 3 μm beam diameter). The chemical composition is given in Table 2. Contents of other elements with atomic numbers higher than carbon are below detection limits.

The empirical formulae calculated on the basis of 18 O apfu for edtollite is: $K_{1.83}Na_{1.07}Cu_{4.88}Zn_{0.06}Fe^{3+}_{0.98}Ti_{0.04}As_{4.03}O_{18}$; and for alumoedtollite is: $K_{2.02}Rb_{0.01}Na_{0.87}Ca_{0.10}Cu_{5.06}Al_{0.72}Fe^{3+}_{0.24}As_{3.99}O_{18}$.

After the grouping of constituents in accordance with the structure data (see below), the empirical formulae could be presented as follows for edtollite: $(K_{1.83}Na_{0.07})_{\Sigma1.90}Na_{1.00}(Cu_{3.90}Zn_{0.06})_{\Sigma3.96}(Cu_{0.98}Fe^{3+}_{0.98}$

Table 6. Coordinates, site multiplicities (Q), site occupancy factors (s.o.f.), equivalent displacement parameters (U_{eq}, in $Å^2$) of atoms, and bond-valence sums (BVS) for edtollite (first line of each row) and alumoedtollite (second line of each row).

Site	Q	x	y	z	s.o.f.	U_{eq}	BVS
K	2	0.2699(6)	0.2207(4)	0.5786(4)	$K_{0.9}$	0.0170(7)	0.95
		0.2685(9)	0.2183(6)	0.5772(5)	K	0.0316(12)	1.10
Na*	1	½	½	0.0	Na	0.049(4)	1.08
					$Na_{0.9}Ca_{0.1}$	0.059(4)	1.16
As1	2	−0.0349(2)	0.26820(15)	0.88942(14)	As	0.0072(3)	4.84
		−0.0357(4)	0.2662(2)	0.8885(2)		0.0125(5)	5.00
As2	2	0.6913(2)	0.30646(15)	0.36986(15)		0.0093(3)	4.99
		0.6896(4)	0.3059(2)	0.3680(2)	As	0.0145(5)	5.08
Cu1	2	0.8148(3)	0.51724(19)	0.73611(18)		0.0116(4)	2.00
		0.8165(5)	0.5162(3)	0.7361(3)	Cu	0.0178(6)	2.01
Cu2	2	0.4319(3)	0.08470(19)	0.90104(19)		0.0119(4)	2.03
		0.4321(4)	0.0843(3)	0.9020(3)	Cu	0.0166(6)	2.01
M*	2	0.8966(3)	0.8872(2)	0.84414(19)	$Fe_{0.602(7)}Cu_{0.398(8)}$	0.0107(4)	2.54
		0.8937(6)	0.8864(3)	0.8433(3)	$Cu_{0.55}Al_{0.35}Fe_{0.1}$	0.0159(7)	2.46
O1	2	−0.0147(16)	0.2794(10)	0.3152(10)	O	0.0111(19)	1.98
		−0.018(3)	0.2734(16)	0.3104(16)		0.022(3)	2.00
O2	2	0.0624(17)	0.0969(11)	0.7838(10)	O	0.015(2)	1.83
		0.062(3)	0.0946(15)	0.7841(15)		0.023(3)	1.90
O3	2	0.1560(17)	0.3033(11)	0.0689(11)	O	0.018(2)**	1.97
		0.155(2)	0.3014(16)	0.0681(14)		0.021(3)	1.97
O4	2	0.2218(17)	0.6656(11)	0.4439(10)	O	0.015(2)	2.05
		0.216(3)	0.6682(15)	0.4484(15)		0.023(3)	2.17
O5	2	0.0769(17)	0.4155(11)	0.8426(11)	O	0.017(2)	2.11
		0.073(2)	0.4141(16)	0.8431(16)		0.021(3)	2.20
O6	2	0.4667(16)	0.1382(10)	0.2869(10)	O	0.0117(19)	1.93
		0.457(3)	0.1428(14)	0.2857(15)		0.020(3)	2.05
O7	2	0.2426(16)	−0.0362(9)	0.9917(9)	O	0.0077(17)	2.04
		0.237(2)	−0.0352(14)	0.9915(13)		0.011(3)**	1.94
O8	2	0.4325(16)	0.5460(10)	0.6710(10)	O	0.014(2)	1.96
		0.436(3)	0.5424(15)	0.6709(15)		0.021(3)	1.94
O9	2	0.6263(16)	0.2537(10)	0.8625(10)	O	0.0105(19)**	2.02
		0.626(3)	0.2553(14)	0.8611(13)		0.015(3)	2.07

*Site occupancy factors for the K site in edtollite and the Na and *M* sites in alumoedtollite were fixed on the last stages of the refinement in accordance with refined numbers of electrons and electron microprobe data; **U_{iso}. Parameters for bond valence calculations were taken from (Brese and O'Keeffe, 1991).

Table 7. Selected interatomic distances (Å) in the structures of edtollite and alumoedtollite.

	Edtollite	Alumoedtollite		Edtollite	Alumoedtollite
K–O4	2.762(9)	2.714(15)	Cu1–O4	1.921(9)	1.943(13)
K–O8	2.812(10)	2.788(14)	Cu1–O5	1.978(9)	1.956(12)
K–O4	2.832(10)	2.844(13)	Cu1–O8	1.982(8)	1.956(13)
K–O9	2.865(9)	2.864(15)	Cu1–O3	2.001(9)	2.005(13)
K–O1	2.889(10)	2.891(14)	Cu1–O1	2.325(9)	2.345(13)
K–O2	2.950(11)	2.951(15)	<Cu1–O>	2.041	2.04
K–O5	2.970(10)	2.976(15)			
K–O6	3.070(9)	3.035(13)	Cu2–O7	1.922(8)	1.932(12)
<K–O>	2.89	2.88	Cu2–O7	1.964(9)	1.955(12)
			Cu2–O9	1.977(9)	1.996(12)
Na–O5	2.283(9) ×2	2.287(12) ×2	Cu2–O2	2.015(8)	2.003(14)
Na–O9	2.388(8) ×2	2.363(12) ×2	Cu2–O6	2.385(9)	2.410(13)
Na–O3	2.790(10) ×2	2.790(13) ×2	Cu2–O3	2.768(9)	2.739(13)
<Na–O>	2.49	2.48	<Cu2–O>	2.172	2.17
As1–O5	1.671(9)	1.656(12)	*M*–O7	1.941(8)	1.925(12)
As1–O9	1.688(8)	1.679(13)	*M*–O6	1.965(8)	1.891(14)
As1–O2	1.714(9)	1.701(13)	*M*–O1	1.985(9)	1.925(14)
As1–O3	1.714(9)	1.705(13)	*M*–O7	1.996(8)	1.965(12)
<As1–O>	1.697	1.69	*M*–O3	2.206(10)	2.183(15)
			M–O2	2.354(10)	2.333(14)
As2–O8	1.647(9)	1.670(13)	<*M*–O>	2.07	2.04
As2–O4	1.689(9)	1.662(13)			
As2–O1	1.702(8)	1.704(13)			
As2–O6	1.703(9)	1.682(12)			
<As2–O>	1.685	1.68			

$Ti_{0.04})_{\Sigma 2.00}O_{1.88}(AsO_4)_{4.03}$; and for alumoedtollite: $(K_{1.98}Rb_{0.01})_{\Sigma 1.99}$ $(Na_{0.87}Ca_{0.10}K_{0.03})_{\Sigma 1.00}Cu_{4.02}(Cu_{1.04}Al_{0.72}Fe^{3+}_{0.24})_{\Sigma 2.00}O_{2.04}(AsO_4)_{3.99}$.

The simplified, end-member formulae are for edtollite $K_2NaCu_5Fe^{3+}O_2(AsO_4)_4$ (which requires Na_2O 2.92, K_2O 8.87, CuO 37.43, Fe_2O_3 7.52, As_2O_5 43.26, total 100.00 wt.%) and for alumoedtollite $K_2NaCu_5AlO_2(AsO_4)_4$ (which requires Na_2O 3.00, K_2O 9.11, CuO 38.48, Al_2O_3 4.93, As_2O_5 44.48, total 100.00 wt.%).

X-ray crystallography

Powder X-ray diffraction (PXRD) data for both minerals were collected with a Rigaku R-AXIS Rapid II single-crystal diffractometer equipped with a cylindrical image plate detector (radius 127.4 mm) using Debye-Scherrer geometry, $CoK\alpha$ radiation (rotating anode with VariMAX microfocus optics), 40 kV, 15 mA, and exposure = 15 min. Angular resolution of the detector is 0.045°2θ (pixel size = 0.1 mm). The data were integrated using the software package *Osc2Tab* (Britvin *et al.*, 2017). The PXRD data for edtollite are given in Table 3 and for alumoedtollite in Table 4. Parameters of triclinic unit cells calculated from the powder data for edtollite are: a = 5.12(1), b = 9.12(2), c = 9.68(2) Å, α = 110.04(5), β = 102.37(4), γ = 92.87(4)° and V = 410.4(5) $Å^3$; and for alumoedtollite are: a = 5.09(1), b = 9.07(2), c = 9.66(2) Å, α = 110.32(7), β = 102.43(7), γ = 92.77(7)° and V = 405.2(6) $Å^3$.

Single-crystal X-ray studies of both new minerals were carried out using an Xcalibur S diffractometer equipped with a CCD
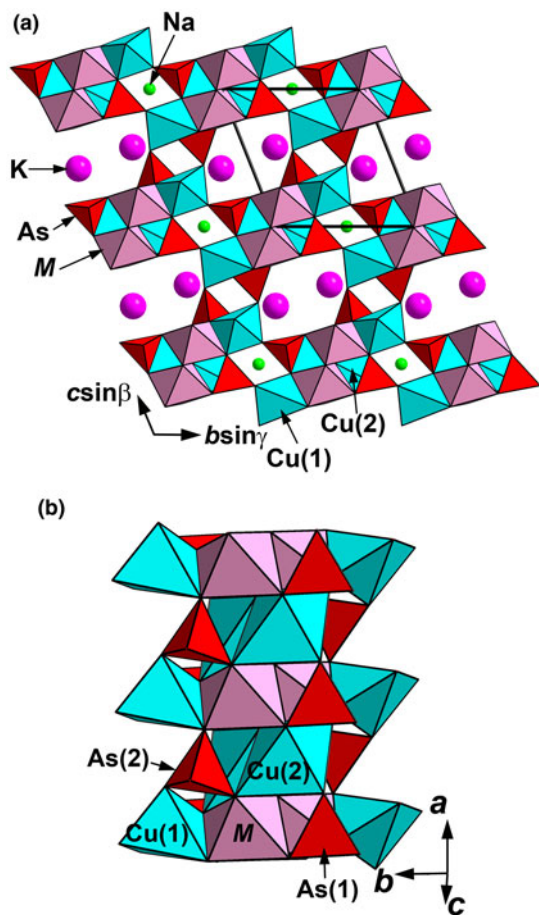
Fig. 6. The crystal structure of edtollite/alumoedtollite projected along the *a* axis (*a*) and its main structural unit, a heteropolyhedral Cu–*M*–As–O column (*b*). For legend see text and Table 6. The unit cell is outlined in (*a*).

detector with a sample-to-detector distance of 45 mm, scan width (Δω) of 1° per frame during the data collection, and an exposure time of 200 s for edtollite and 300 s for alumoedtollite. The crystal structures were solved by direct methods and refined with the use of *SHELX-97* software package (Sheldrick, 2008) using the neutral atom scattering factors. The refinement was performed in aniso-tropic approximation for all atoms except O3 and O9 sites in edtollite and O7 in alumoedtollite. Site occupancy factors for the K site in edtollite and Na and *M* sites in alumoedtollite were refined and fixed on the last cycles of the refinement in accordance with refined numbers of electrons, electron micro-probe data and the requirement of charge-balanced formulae. The crystal data, data collection information and structure refine-ment details for edtollite and alumoedtollite are given in Table 5, fractional atomic coordinates and displacement parameters of atoms and bond-valence sums in Table 6, and selected interatomic distances in Table 7. Detailed bond-valence calculations are given in Supplementary material Tables S1a and S1b (see below).

Crystal structure

Edtollite and alumoedtollite show a novel structure type. They are isostructural and, thus, we give the shared crystal-structure draw-ings in Figs 6 and 7*a*, and use the generalised term 'edtollites' below if both minerals are meant. Their crystal structure

(Fig. 6*a*) is based on the heteropolyhedral pseudo-framework hav-ing, as the main structural unit, a heteropolyhedral column (Fig. 6*b*) elongated along *a* and built as follows: Cu2-centred dis-torted octahedra with [4+1+1] Cu^{2+} coordination of which is four short Cu2–O bonds, one elongated bond and one strongly elon-gated bond; distorted octahedra MO_6 with [4+2] coordination of which is four short *M*–O bonds and two elongated bonds; dis-torted Cu1-centred square pyramids; and isolated AsO_4 tetra-hedra. $Cu2O_6$ and MO_6 octahedra compose the axial part of the column (Fig. 7*a*). $Cu2O_6$ octahedra are characterised by strong Jahn–Teller distortion, but this is not so significant (Table 7) for MO_6 octahedra. Cu1-centred polyhedra share common edges with MO_6 octahedra (Fig. 6*a*). The formula of the heteropolyhedral pseudo-framework of both minerals can be written as $[Cu_4M_2O_2(AsO_4)_4]^{3-}$. Large cations K^+ and Na^+ are located in channels of the pseudo-framework. In detail, K occurs in wide chan-nels and the centre of eight-fold polyhedra, whereas Na, along with minor Ca admixtures, is in the centre of distorted octahedra in narrow channels (Fig. 6*a*) that are isolated from each other.

Interatomic distances (Table 7) and bond-valence calculations (weighted bond-valence sums: Bosi, 2014) for the *M* site (Table 6) clearly indicate the occurrence of both divalent (Cu^{2+}) and triva-lent (Fe^{3+} and Al) cations in approximately equal amounts. The refined number of electrons in the *M* site in alumoedtollite (e_{ref}^- = 22.9) clearly shows that Al occurs there. The presence of Fe^{3+} in edtollites is consistent with strongly oxidising conditions in the Arsenatnaya fumarole (Pekov *et al.*, 2014*a*, 2018*b*).

The general crystal chemical formula of edtollites is $^K K_2 {}^{Na} Na$ $^{Cu(1-2)} Cu_4 {}^M (CuM^{3+})O_2 (^{As(1-2)} AsO_4)_4$, where the superscript sym-bols show structure positions (Table 6); M^{3+} = Fe or Al in edtollite or alumoedtollite, respectively. The distribution of cations in the empirical formulae reported above is made in accordance with this formula. The species-defining feature that causes a difference between edtollite and alumoedtollite is in the occupancy of the *M* site: for their end-members, it should be written as (CuAl) and (CuFe³⁺), respectively. Both electron microprobe and structure refinement data show that in edtollite the content of the *M* site is ($Fe_{0.6}^{3+} Cu_{0.4}$) while in alumoedtollite it is ($Cu_{0.55} Al_{0.35} Fe_{0.1}$). Thus these minerals are different in terms of both approaches, (1) using general predominance of a constituent in a site (*M* is Fe^{3+}-dominant in edtollite and Cu^{2+}-dominant in alumoedtollite) and (2) using the valency-imposed double site-occupancy principle: ($Cu^{2+}Fe^{3+}$) in edtollite and ($Cu^{2+}Al^{3+}$) in alumoedtol-lite. The latter approach is in use as a nomenclature rule accepted by the IMA CNMNC for such cases (Hatert and Burke, 2008: pp. 719–720). In particular, the name alumoedtollite was given in accordance with this rule. The simplified crystal-chemical formulae of edtollite and alumoedtollite can be written as $K_2NaCu_4(CuFe^{3+})O_2(AsO_4)_4$ and $K_2NaCu_4(CuAl)O_2(AsO_4)_4$, respectively.

The presence of admixed Ca in the *Na* site in alumoedtollite allows the full substitution of Na for Ca in this position to be assumed. It could result in the absence of a trivalent cation in the *M* site with the formation of the hypothetic phase with the end-member formula $K_2CaCu_6O_2(AsO_4)_4$, a dimorph of shchur-ovskyite (see below) with the edtollite-type structure. Moreover, both *Na* and *M* sites share the oxygen atom O3 and this bond is the longest for the Na-centred polyhedron and one of the long-est for the *M* polyhedron. Possible dominance of Ca at the *Na* site probably would reduce the Na(Ca)–O3 distance, while the *M*–O3 becoming longer would be in a good accordance with the domin-ance of Cu at the *M* site.
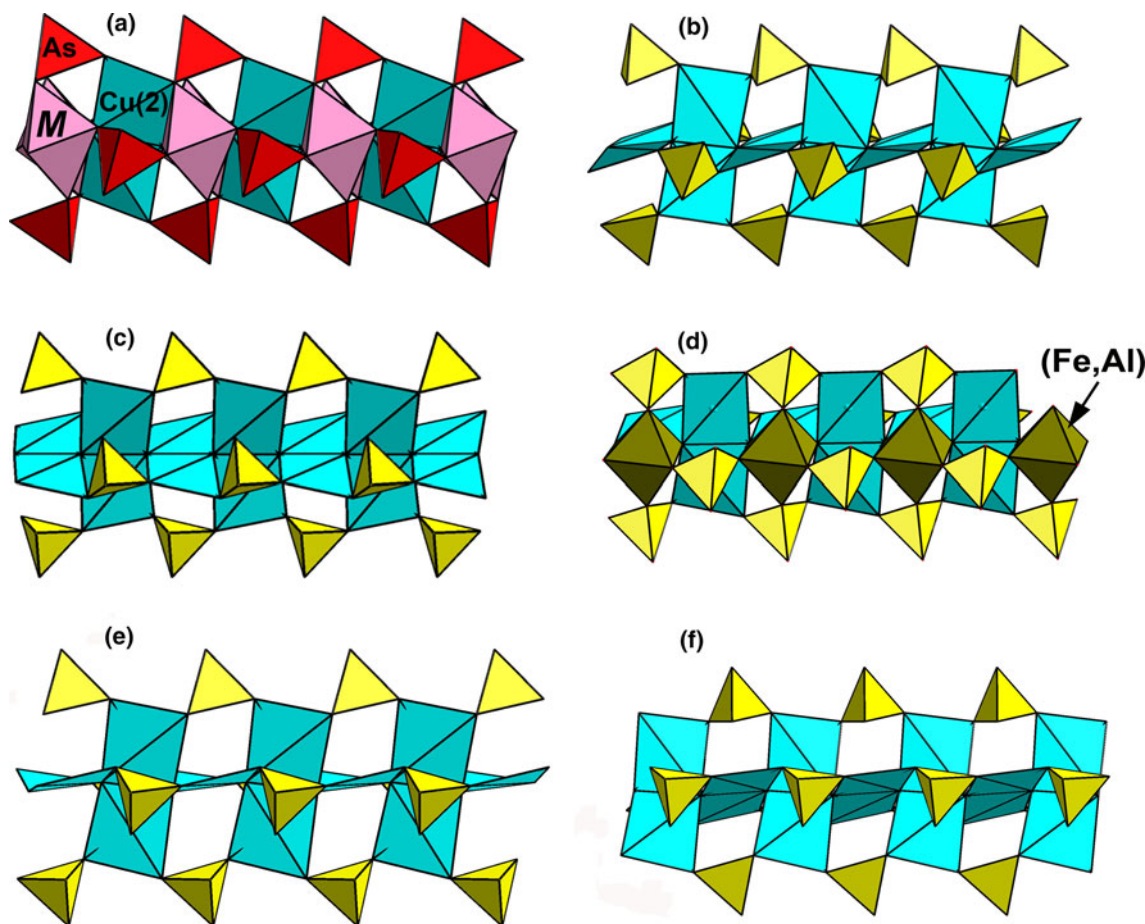
Fig. 7. The heteropolyhedral chains in edtollite/alumoedtollite (our data; only the axial part of the column presented in Fig. 6b is shown there) (*a*); and structurally related sulfates: eleomelanite (*b*: our data); piypite (*c*: drawn using data from Effenberger and Zemann, 1984); klyuchevskite (*d*: drawn using data by Gorskaya *et al.*, 1992); wulffite (*e*); and parawulffite (*f*) (drawn using data from Pekov *et al.*, 2014*c*). Cu-centred polyhedra are blue, SO₄ tetrahedra are yellow.

Relationship to other minerals

The axial part of the above-discussed heteropolyhedral column in edtollites formed by Cu2- and *M*-centred octahedra and AsO_4 tetrahedra (Fig. 7*a*) is close to that found in several oxysulfates, namely eleomelanite $(K_2Pb)Cu_4O_2(SO_4)_4$ (IMA2015-118, Pekov *et al.*, 2016*b*), klyuchevskite $K_3Cu_3Fe^{3+}O_2(SO_4)_4$ (Gorskaya *et al.*, 1992), alumoklyuchevskite $K_3Cu_3AlO_2(SO_4)_4$ (Krivovichev *et al.*, 2009; Siidra *et al.*, 2017), wulffite $K_3NaCu_4O_2(SO_4)_4$, parawulffite $K_5Na_3Cu_8O_4(SO_4)_8$ (Pekov *et al.*, 2014*c*), piypite $K_8Cu_9O_4(SO_4)_8Cl_2 = K_8Cu_8O_4(SO_4)_8 \cdot CuCl_2$ (Effenberger and Zemann, 1984) (Fig. 7), and two synthetic piypite-like phases $K_4Cu_4O_2(SO_4)_2 \cdot KCl$ (Effenberger, 1985) and $Na_4Cu_4O_2(SO_4)_2 \cdot$ *Me*Cl (*Me* = Na, Cu or □) (Kahlenberg *et al.*, 2000). Structures of the above-listed minerals are shown in Supplementary material Fig. S1; for better clarity and comparison all Cu-centred polyhedra are shown as approximately planar squares whereas elongated Cu–O bonds are not included in the polyhedra, and only the axial part of the heteropolyhedral column for edtollites is shown in polyhedral presentation whereas Cu1 sites are given as circles. Close topology of the heteropolyhedral chains in edtollites, eleomelanite, piypite, wulffite, parawulffite, klyuchevskite and alumoklyuchevskite causes a comparable value of the unit-cell parameter in the direction parallel to the chain: 5.09 Å in alumoedtollite, 5.12 Å in edtollite and 4.9–5.0 Å in the sulfates.

Edtollite, ideally $K_2NaCu_5Fe^{3+}O_2(AsO_4)_4$, and alumoedtollite, ideally $K_2NaCu_5AlO_2(AsO_4)_4$, demonstrate the same stoichiometry and the same ratios between large (K, Na or Ca) and medium-size (Cu, Fe or Al) metal cations as two other arsenate minerals closely associated with edtollites, namely shchurovskyite $K_2CaCu_6O_2(AsO_4)_4$ and dmisokolovite $K_3Cu_5AlO_2(AsO_4)_4$ (Pekov *et al.*, 2015*c*). The latter and alumoedtollite have very similar idealised formulae, with the only difference being in the large-cation part: K_3 in dmisokolovite and K_2Na in alumoedtollite. However, the structural difference between edtollites and the pair of arsenates closely related to each other – shchurovskyite and dmisokolovite – is significant. Edtollites differ from shchurovskyite and dmisokolovite in atomic arrangement that causes strong differences in unit-cell dimensions and PXRD patterns. These structure features also strongly influence the physical properties: shchurovskyite and dmisokolovite are transparent green minerals with a vitreous lustre while edtollite is brown–black and alumoedtollite is bronze coloured, both with a semi-metallic lustre (Table 8).

It is worth noting the crystal chemical relationship (see Figs 7 and S1) between the oxyarsenate pair edtollite $K_2NaCu_5Fe^{3+}O_2(AsO_4)_4$–alumoedtollite $K_2NaCu_5AlO_2(AsO_4)_4$ and the oxysulfate pair klyuchevskite $K_3Cu_3Fe^{3+}O_2(SO_4)_4$–alumoklyuchevskite $K_3Cu_3AlO_2(SO_4)_4$ occurring in the same Arsenatnaya fumarole.

Table 8. Comparative data of four arsenates with the same stoichiometry: edtollite, alumoedtollite, dmisokolovite and shchurovskyite.

Mineral	Edtollite	Alumoedtollite	Dmisokolovite	Shchurovskyite
Idealised formula	$K_2NaCu_5Fe^{3+}O_2(AsO_4)_4$	$K_2NaCu_5AlO_2(AsO_4)_4$	$K_3Cu_5AlO_2(AsO_4)_4$	$K_2CaCu_6O_2(AsO_4)_4$
Crystal system	Triclinic	Triclinic	Monoclinic	Monoclinic
Space group	$P\bar{1}$	$P\bar{1}$	$C2/c$	$C2$
a, Å	5.1168(6)	5.0904(11)	17.0848(12)	17.2856(9)
b, Å	9.1241(12)	9.0778(14)	5.7188(4)	5.6705(4)
c, Å	9.6979(14)	9.6658(2)	16.5332(12)	8.5734(6)
α, °	110.117(13)	110.334(17)		
β, °	102.454(12)	102.461(19)	91.716(6)	92.953(6)
γ, °	92.852(11)	92.788(15)		
V, Å³	411.32(9)	404.88(14)	1614.7(2)	839.24(9)
Z	1	1	4	2
The strongest reflections of the PXRD pattern: d, Å – I	8.79–92; 7.63–41; 5.22–44; 3.427–100; 3.148–64; 2.851–65; 2.569–77; 2.551–40; 2.528–38	8.78–81; 7.62–67; 5.20–48; 3.418–100; 3.147–52; 2.843–51; 2.558–58; 2.544–65; 2.528–52	8.34–95; 6.034–40; 5.433–84; 3.274–45; 2.921–66; 2.853–58; 2.733–100; 2.451–47; 2.366–45	8.61–100; 5.400–32; 3.759–28; 2.974–32; 2.842–47; 2.757–63; 2.539–26; 2.373–36; 2.297–31
Transparency; colour; lustre	translucent to almost opaque; brown–black to black; semi-metallic	translucent to almost opaque; bronze coloured; semi-metallic	transparent; bright emerald-green; vitreous	transparent; olive-green to olive drab; vitreous
Source	This work	This work	Pekov et al. (2015c)	Pekov et al. (2015c)
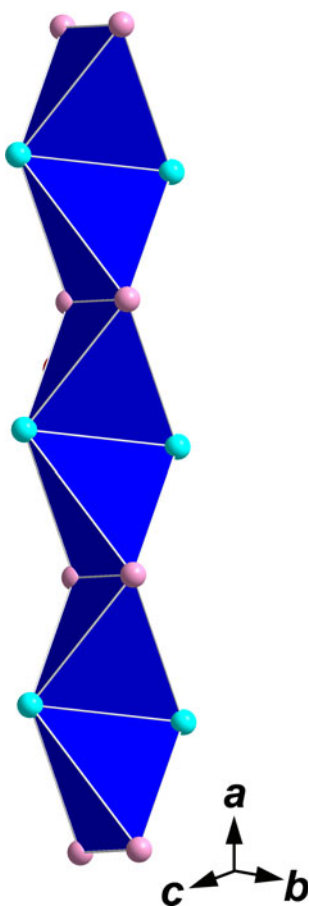
Fig. 8. Chain $[O_2Cu_2M_2]^\infty$ formed by oxocentred tetrahedra OCu_2M_2 in the crystal structure of edtollite/alumoedtollite. Turquoise-coloured circles are Cu^{2+} cations and pink circles are M cations (see Table 6).

The crystal structure of edtollites could also be described in terms of anion-centred (oxocentred) tetrahedra (Krivovichev et al., 2013). O7 atoms are bonded only with Cu2 and M to form the $[O_2Cu_2M_2]^\infty$ chains built by edge-sharing OCu_2M_2 tetrahedra and running along the a axis (Fig. 8). Similar chains

built by tetrahedra $[OFeCu_3]$ and $[OAlCu_3]$ were described in klyuchevskite (Gorskaya et al., 1992) and alumoklyuchevskite (Krivovichev et al., 2009), respectively; this feature emphasises the above-mentioned similarity of edtollites and these sulfates. Topologically the same chains built by OCu_4 tetrahedra were found in eleomelanite (Pekov et al., 2016b), piypite (Effenberger and Zemann, 1984), its synthetic sodium analogue Na_2Cu_2O $(SO_4)\cdot MCl$ (M = Na, Cu or $\square$) (Kahlenberg et al., 2000), coparsite, $Cu_4O_2[(As,V)O_4]Cl$ (Starova et al., 1998), wulffite and para-wulffite (Pekov et al., 2014c). Unlike them, in shchurovskyite and dmisokolovite the motif of oxocentred tetrahedra is represented by isolated (from each other) dimers, $[O_2Cu_6]$ and $[O_2AlCu_5]$, respectively (Pekov et al., 2015c).

Supplementary material. To view supplementary material for this article, please visit https://doi.org/10.1180/mgm.2018.155

References

Agilent Technologies (2014) *CrysAlisPro Software system, version 1.171.37.35*. Agilent Technologies UK Ltd, Oxford, UK.

Bosi F. (2014) Bond valence at mixed occupancy sites. I. Regular polyhedra. *Acta Crystallographica*, **B70**, 864–870.

Brese N.E. and O`Keeffe M. (1991) Bond-valence parameters for solids. *Acta Crystallographica*, **B47**, 192–197.

Britvin S.N., Dolivo-Dobrovolsky D.V. and Krzhizhanovskaya M.G. (2017) Software for processing the X-ray powder diffraction data obtained from the curved image plate detector of Rigaku RAXIS Rapid II diffractometer. *Zapiski Rossiiskogo Mineralogicheskogo Obshchestva*, **146**, 104–107 [in Russian].

Effenberger H. (1985) Zur chemischen Zusammensetzung von Caratiit. *Mitteilungen der Österreichischen Mineralogischen Gesellschaft*, **130**, 29–31.

Effenberger H. and Zemann J. (1984) The crystal structure of caratiite. *Mineralogical Magazine*, **48**, 541–546.

Gorskaya M.G., Filatov S.K., Rozhdestvenskaya I.V. and Vergasova L.P. (1992) The crystal structure of klyuchevskite, $K_3Cu_3(Fe,Al)O_2(SO_4)_4$, a new mineral from Kamchatka volcanic sublimates. *Mineralogical Magazine*, **56**, 411–416.

Hatert F. and Burke E.A.J. (2008) The IMA–CNMNC dominant-constituent rule revisited and extended. *The Canadian Mineralogist*, **46**, 717–728.

Kahlenberg V., Piotrowski A. and Giester G. (2000) Crystal structure of $Na_4[Cu_4O_2(SO_4)_4] \cdot MeCl$ (Me: Na, Cu, □) – the synthetic Na-analogue of piypite (caratiite). *Mineralogical Magazine*, **64**, 1099–1108.

Krivovichev S.V., Filatov S.K. and Cherepansky P.N. (2009) The crystal structure of alumoklyuchevskite, $K_3Cu_3AlO_2(SO_4)_4$. *Geology of Ore Deposits*, **51**, 656–662.

Krivovichev S.V., Mentre O., Siidra O.I., Colmont M. and Filatov S.K. (2013) Anion-centered tetrahedra in inorganic compounds. *Chemical Reviews*, **113**, 6459–6535.

Pekov I.V., Zubkova N.V., Yapaskurt V.O., Belakovskiy D.I., Lykova I.S., Vigasina M.F., Sidorov E.G. and Pushcharovsky D.Yu. (2014a) New arsenate minerals from the Arsenatnaya fumarole, Tolbachik volcano, Kamchatka, Russia. I. Yurmarinite, $Na_7(Fe^{3+},Mg,Cu)_4(AsO_4)_6$. *Mineralogical Magazine*, **78**, 905–917.

Pekov I.V., Zubkova N.V., Yapaskurt V.O., Belakovskiy D.I., Vigasina M.F., Sidorov E.G. and Pushcharovsky D.Yu. (2014b) New arsenate minerals from the Arsenatnaya fumarole, Tolbachik volcano, Kamchatka, Russia. II. Ericlaxmanite and kozyrevskite, two natural modifications of $Cu_4O(AsO_4)_2$. *Mineralogical Magazine*, **78**, 1527–1543.

Pekov I.V., Zubkova N.V., Yapaskurt V.O., Belakovskiy D.I., Chukanov N.V., Lykova I.S., Saveliev D.P., Sidorov E.G. and Pushcharovsky D.Yu. (2014c) Wulffite, $K_3NaCu_4O_2(SO_4)_4$, and parawulffite, $K_5Na_3Cu_8O_4(SO_4)_8$, two new minerals from fumarole sublimates of the Tolbachik volcano, Kamchatka, Russia. *The Canadian Mineralogist*, **52**, 699–716.

Pekov I.V., Britvin S.N., Yapaskurt V.O., Polekhovsky Y.S., Krivovichev S.V., Vigasina M.F. and Sidorov E.G. (2015a) Arsmirandite, IMA 2014-081. CNMNC Newsletter No. 23, February 2015, page 57; *Mineralogical Magazine*, **79**, 51–58.

Pekov I.V., Zubkova N.V., Yapaskurt V.O., Belakovskiy D.I., Vigasina M.F., Sidorov E.G. and Pushcharovsky D.Yu. (2015b) New arsenate minerals from the Arsenatnaya fumarole, Tolbachik volcano, Kamchatka, Russia. III. Popovite, $Cu_5O_2(AsO_4)_2$. *Mineralogical Magazine*, **79**, 133–143.

Pekov I.V., Zubkova N.V., Belakovskiy D.I., Yapaskurt V.O., Vigasina M.F., Sidorov E.G. and Pushcharovsky D.Yu. (2015c) New arsenate minerals from the Arsenatnaya fumarole, Tolbachik volcano, Kamchatka, Russia. IV. Shchurovskyite, $K_2CaCu_6O_2(AsO_4)_4$, and dmisokolovite, $K_3Cu_5AlO_2(AsO_4)_4$. *Mineralogical Magazine*, **79**, 1737–1753.

Pekov I.V., Yapaskurt V.O., Britvin S.N., Zubkova N.V., Vigasina M.F. and Sidorov E.G. (2016a) New arsenate minerals from the Arsenatnaya fumarole, Tolbachik volcano, Kamchatka, Russia. V. Katiarsite, $KTiO(AsO_4)$. *Mineralogical Magazine*, **80**, 639–646.

Pekov I.V., Zubkova N.V., Agakhanov A.A., Chukanov N.V., Belakovskiy D.I., Sidorov E.G., Britvin S.N. and Pushcharovsky D.Yu. (2016b) Eleomelanite,

IMA 2015–118. CNMNC Newsletter No. 30, April 2016, page 412. *Mineralogical Magazine*, **80**, 407–413.

Pekov I.V., Zubkova N.V., Agakhanov A.A., Pautov L.A., Vigasina M.F., Sidorov E.G., Ksenofontov D.A., Britvin S.N. and Pushcharovsky D.Y. (2016c) Edtollite, IMA 2016-010. CNMNC Newsletter No. 31, June 2016, page 696; *Mineralogical Magazine*, **80**, 691–697.

Pekov I.V., Zubkova N.V., Yapaskurt V.O., Polekhovsky Yu.S., Vigasina M.F., Belakovskiy D.I., Britvin S.N., Sidorov E.G. and Pushcharovsky D.Yu. (2016d) New arsenate minerals from the Arsenatnaya fumarole, Tolbachik volcano, Kamchatka, Russia. VI. Melanarsite, $K_3Cu_7Fe^{3+}O_4(AsO_4)_4$. *Mineralogical Magazine*, **80**, 855–867.

Pekov I.V., Yapaskurt V.O., Belakovskiy D.I., Vigasina M.F., Zubkova N.V. and Sidorov E.G. (2017a) New arsenate minerals from the Arsenatnaya fumarole, Tolbachik volcano, Kamchatka, Russia. VII. Pharmazincite, $KZnAsO_4$. *Mineralogical Magazine*, **81**, 1001–1008.

Pekov I.V., Zubkova N.V., Agakhanov A.A., Sidorov E.G., Ksenofontov D.A., Britvin S.N. and Pushcharovsky D.Y. (2017b) Alumoedtollite, IMA2017-020. CNMNC Newsletter No. 38, August 2017, page 1034; *Mineralogical Magazine*, **81**, 1033–1038.

Pekov I.V., Zubkova N.V., Agakhanov A.A., Yapaskurt V.O., Chukanov N.V., Belakovskiy D.I., Sidorov E.G. and Pushcharovsky D.Yu. (2018a) New arsenate minerals from the Arsenatnaya fumarole, Tolbachik volcano, Kamchatka, Russia. VIII. Arsenowagnerite, $Mg_2(AsO_4)F$. *Mineralogical Magazine*, **82**, 877–888.

Pekov I.V., Koshlyakova N.N., Zubkova N.V., Lykova I.S., Britvin S.N., Yapaskurt V.O., Agakhanov A.A., Shchipalkina N.V., Turchkova A.G. and Sidorov E.G. (2018b) Fumarolic arsenates – a special type of arsenic mineralization. *European Journal of Mineralogy*, **30**, 305–322.

Pekov I.V., Zubkova N.V., Agakhanov A.A., Belakovskiy D.I., Vigasina M.F., Yapaskurt V.O., Sidorov E.G., Britvin S.N. and Pushcharovsky D.Yu. (2018c) New arsenate minerals from the Arsenatnaya fumarole, Tolbachik volcano, Kamchatka, Russia. IX. Arsenatrotitanite, $NaTiO(AsO_4)$. *Mineralogical Magazine*, **82**, DOI: https://doi.org/10.1180/mgm.2018.134

Sheldrick G.M. (2008) A short history of *SHELX*. *Acta Crystallographica*, **A64**, 112–122.

Siidra O.I., Nazarchuk E.V., Zaitsev A.N., Lukina E.A., Avdontseva E.Y., Vergasova L.P., Vlasenko N.S., Filatov S.K., Turner R. and Karpov G.A. (2017) Copper oxosulphates from fumaroles of Tolbachik volcano: puninite, $Na_2Cu_3O(SO_4)_3$ – a new mineral species and structure refinements of kamchatkite and alumoklyuchevskite. *European Journal of Mineralogy*, **29**, 499–510.

Starova G.L., Krivovichev S.V. and Filatov S.K. (1998) Crystal chemistry of inorganic compounds based on chains of oxocentered tetrahedra. II. The crystal structure of $Cu_4O_2[(As,V)O_4]Cl$. *Zeitschrift für Kristallographie*, **213**, 650–653.